

Author Manuscript

Immunoisolating poly(ethylene glycol) based capsules support ovarian tissue survival to restore endocrine function

James R. Day^a, Anu David^a, Alexa L. Cichon^c, Tanay Kulkarni^a, Marilia Cascalho^{d,e}, Ariella Shikanov^{a,b}

^aDepartment of Biomedical Engineering, University of Michigan, Ann Arbor, USA

^bDepartment of Macromolecular Science & Engineering, University of Michigan, Ann Arbor, USA

^cDepartment of Chemical Engineering, University of Michigan, Ann Arbor, USA

^dDepartment of Surgery, University of Michigan, Ann Arbor, USA

^eDepartment of Microbiology & Immunology, University of Michigan, Ann Arbor, USA

This is the author manuscript accepted for publication and has undergone full peer review but has not been through the copyediting, typesetting, pagination and proofreading process, which may lead to differences between this version and the [Version of record](#). Please cite this article as [doi:10.1002/jbm.a.36338](https://doi.org/10.1002/jbm.a.36338).

ABSTRACT

A common irreversible adverse effect of life-saving anticancer treatments is loss of gonadal endocrine function and fertility, calling for a need to focus on post-treatment quality of life. Here, we investigated the use of poly(ethylene glycol)-vinyl sulfone based capsules to support syngeneic donor ovarian tissue for restoration of endocrine function in mice. We designed a dual immunisolating capsule (PEG-Dual) by tuning the physical properties of the PEG hydrogels and combining proteolytically degradable (PEG-PD) and non-degradable (PEG-NPD) layers to meet the numerous requirements for encapsulation and immunoisolation of ovarian tissue, such as nutrient diffusion and tissue expansion. Tuning the components of the PEG-Dual capsule to have similar physical properties allowed for concentric encapsulation. Upon implantation, the PEG-based capsules supported ovarian tissue survival and led to a significant decrease in FSH levels 60 days post-implantation. Mice that received the implants resumed regular estrous cycle activity and follicle development in the implanted grafts. The PEG-Dual capsule provided an environment conducive for tissue survival, while providing a barrier to the host environment. This study demonstrated for the first time that immunisolating PEG-VS capsules can support ovarian follicular development resulting in the restoration of ovarian endocrine function and can be applied to future allogeneic studies.

KEY WORDS

Endocrine function restoration, poly (ethylene glycol), hydrogel, immunoisolation

INTRODUCTION

Loss of gonadal endocrine function and fertility in cancer patients undergoing chemo- and radiotherapy is a common irreversible consequence of these lifesaving therapies¹⁻⁶.

With improved survival rates of up to 80%, survivors of childhood cancer are a rapidly growing population, necessitating a shift in focus from simply survival to quality of life post-treatment. Abnormal puberty, osteopenia, muscle wasting, cardiovascular disease, frailty, sterility and risk of premature death all stem from impaired gonadal function⁷⁻¹⁰.

The restoration of reproductive and endocrine function is uniquely challenging due to the limited and non-renewable ovarian reserve. Cryopreservation of ovarian or testicular tissue obtained prior to exposure to gonadotoxic treatments, with subsequent implantation in survivors can restore both fertility and endocrine function, but the risk of re-introducing malignant cells present in the ovarian tissue limits its translation to the clinic¹¹⁻¹³.

To avoid this risk, implantation of the donor ovarian tissue encapsulated in an immunoisolating capsule has the potential to restore ovarian endocrine function by secreting the gonadal hormones, while eliminating the risk of reseeding cancer cells and the need for immunosuppressant therapy.

Implantation of hormone secreting cells, such as pancreatic islets, in immunoisolating capsules has been investigated for treating Type I diabetes¹⁴⁻¹⁷. For this purpose, hormone secreting cells are encapsulated in a semi-permeable membrane that prevents or attenuates the interaction between the encapsulated allogeneic cells or tissue and the host immune system, while allowing diffusion of nutrients and waste¹⁸.

Ovarian follicles, which are the functional hormone secreting units of the ovary, are

similar to islets in that they synthesize and secrete hormones in response to circulating stimuli, in this case follicle stimulating hormone (FSH); however, unlike islets, ovarian follicles are dynamic in growth. At the beginning of each cycle only a small portion of follicles activates and enters the growing pool. The growing follicles undergo a multiple fold volumetric expansion, which when encapsulated in an immunisolating capsule must be accommodated by a degradable matrix that mirrors and allows the follicle expansion. Furthermore, follicles are avascular and relatively resistant to hypoxia, allowing them to survive and function with diffusion through the encapsulating matrix being the only mechanism to supply oxygen and nutrients.

We have reported earlier that hydrogels prepared with poly(ethylene glycol) vinyl sulfone (PEG-VS) and crosslinked with proteolytically sensitive peptides supported follicle development *in vitro* and *in vivo*^{19,20}. For the purposes of immunoisolation, we investigated whether the tunable properties of PEG hydrogels and inert non-immunogenic interface with the host^{21,22} can match the requirements to allow follicle expansion while preventing infiltration of the cells from the host and immune reaction. We encapsulated syngeneic ovarian tissue in three different PEG-VS constructs: a non-degradable photo-polymerized PEG-VS hydrogel (PEG-NPD), a proteolytically degradable PEG-VS hydrogel (PEG-PD), and a dual PEG-VS hydrogel (PEG-Dual) construct containing a proteolytically degradable PEG-VS core with a non-degradable PEG-VS shell (Scheme 1). The objectives of this study were to: 1) answer the question whether the viscoelastic properties of a non-degradable PEG-VS hydrogel are sufficient to allow follicle expansion; 2) create a dual construct with a degradable core and non-degradable shell

with controlled physical properties to match follicle expansion; and 3) to identify the PEG-VS-based hydrogel construct that supports ovarian tissue survival and function, leading to ovarian endocrine function restoration.

MATERIALS AND METHODS

Hydrogel Preparation

To form the PEG-NPD hydrogel network, 4-arm poly (ethylene glycol) vinyl sulfone (PEG-VS, 20kDa, JenKem Technology, Beijing, China) is dissolved in a solution containing sterile D-PBS (pH 7.4) and 0.4 mg/100 μ L Irgacure 2959 (Ciba, Switzerland, MW=224.3) to create a concentration of 5% w/v. Irgacure 2959 is the photo-initiator of choice as it has been demonstrated to be biocompatible across multiple cell lines²³. Further, N-vinyl-2-pyrrolidone (NVP) (Sigma-Aldrich, St. Louis, USA) is added at a final concentration of 0.1%, as NVP has been demonstrated to enhance gelation without impacting cytocompatibility²⁴. To induce cross-linking, the precursor solution is exposed to UV light at a constant intensity (1090 μ W/cm² at a distance of 4 cm).

The PEG-PD hydrogels are formed via Michael-type addition through the inclusion of a plasmin sensitive tri-functional peptide sequence (Ac-GCYK↓NSGCK↓NSCG, MW 1525.69 g/mol, >90% Purity, CelTek, ↓ indicates the cleavage site). Briefly, to prepare the gels, 8-arm PEG-VS (40kDa, JenKem Technology, Beijing, China) is dissolved in an isotonic HEPES buffer (HEPES 0.05M, pH=7.4) to create a final concentration of 5 or 10% w/v and YKNS was added, such that the molar ratio of –SH and –VS groups was 1:1.

The PEG-Dual hydrogel construct contains a proteolytically degradable core with a non-degradable outer shell. To manufacture the dual PEG hydrogel, a 4 μL degradable core (5% w/v PEG-VS) is formed via the aforementioned technique for the degradable 8-arm PEG-VS hydrogel. Immediately after 5 minutes of gelation, the degradable hydrogel bead is transferred over and placed in the center of a 10 μL bead of the non-degradable precursor solution. The PEG-Dual construct is then exposed to a constant intensity (1090 $\mu\text{W}/\text{cm}^2$ at a distance of 4 cm) for 6 minutes creating the non-degradable outer shell of the hydrogel (Scheme 1).

Swelling Ratio

5% w/v PEG-NPD and PEG-PD hydrogels were tested. The PEG-NPD gels were exposed to UV light for 6 minutes and were submerged in DPBS for 24 hours. Similarly, the PEG-PD gels formed for 5 minutes after the introduction of YKNS; thereafter the reaction was quenched by submerging the gels in DPBS and remained there for 24 hours. After 24 hours, excess DPBS was removed and the swollen mass of the hydrogels was obtained. Gels were then removed from solution and allowed to dry at room temperature. Larger volumes were used to minimize error from weighing. The mass swelling ratio (Q_m) was determined by dividing the mass of the swollen gels (M_s) by the mass of the dry gels (M_d)²⁵.

Rheology

The storage modulus (G') and loss modulus (G'') was investigated for two PEG constructs—5% PEG-NPD and 5% PEG-PD. The gels were prepared and swollen in DPBS

overnight. A TA HR-2 rheometer (TA Instruments, USA) equipped with 20 mm parallel plates and a Peltier stage was used for this purpose. To ensure the hydrogel was the same size as the geometry, 1 mm thick hydrogel slabs were made and a 20mm diameter disc was punched out. A constant strain rate of 5% was kept for all samples and the storage modulus was obtained by performing an angular frequency sweep from 0.1 to 10 rad/s.

Ovariectomies in recipient mice

Before any surgical procedure, preemptive analgesics were administered. To induce infertility, bilateral ovariectomies were performed on 12-16 week old adult female mice (B6CBAF1). All procedures (PRO00005750) followed the IACUC guidelines for survival surgery in rodents and the IACUC Policy on Analgesic Use in Animals Undergoing Surgery. Briefly, the female was anesthetized by isoflurane, Carprofen (Rimadyl, Zoetis, USA) was administered, and a midline incision was made in the abdominal wall. Using an abdomen retractor, the intraperitoneal space was exposed, and the ovaries were removed, leaving the remainder of the reproductive tract. The muscle and skin layer of the abdominal wall were closed with 5/0 absorbable sutures (AD Surgical, USA). The animal recovered in a clean warmed cage. Post-surgery, animals received analgesia for at least 24 hours or as needed.

Ovarian tissue encapsulation in PEG hydrogels

Ovaries were collected from 6-8 days old B6CBAF1 female pups. These pups are

genetically matched to the receiving host. The collected ovaries were transferred to Leibovitz L-15 media (Sigma-Aldrich, USA) and dissected into 2 pieces. The ovarian tissue pieces were then transferred into maintenance media (α -MEM) and placed into incubator set to 5% CO₂. For encapsulation in PEG-NPD, the ovarian tissue was transferred into a 10 μ L droplet of the precursor solution (5% w/v PEG-VS, .4% Irgacure 2959, .1% NVP) and exposed to UV light. For encapsulation in the PEG-PD, the ovarian tissue was transferred into a 10 μ L droplet of the plasmin sensitive tri-functional peptide and PEG-VS precursors' solution. The droplet was allowed to crosslink for 5 minutes and then was quenched in maintenance media. For the PEG-Dual hydrogel encapsulation, the tissue was first encapsulated in a 4 μ L PEG-PD gel and was then placed in the center of a 10 μ L bead of PEG-NPD and exposed to UV light. All constructs were imaged immediately after encapsulation of the tissue.

Implantation of immunoisolating capsules in mice

To investigate the survival and function of the ovarian tissue encapsulated in immunoisolation capsules we implanted subcutaneously immunoisolating capsules in the ovariectomized mice. Briefly, a small incision was made on the dorsal side of the anesthetized mice and two constructs (PEG-NPD, PEG-PD, or PEG-Dual) with encapsulated ovarian tissue were implanted subcutaneously and the skin was closed using 5/0 absorbable sutures. The mice received analgesia for at least 24 hours after surgery or as needed. Mice were euthanized at pre-determined end time points (7, 30, and 60 days post-operation).

Serum Hormone analysis

Blood was collected from the lateral tail vein at designated time points with a 5^{3/4} glass Pasteur pipette up to the time of sacrifice. After collection, all samples were stored at 4°C overnight, then centrifuged for 10 minutes at 10,000 rpm and the collected serum was stored at -20°C. The samples were analyzed for mouse FSH using a radio-immunoassay (Ligand Assay and Analysis Core Facility, University of Virginia Center for Research in Reproduction). The core at the University of Virginia used mouse FSH reference preparation AFP5308D for assay standards and mouse FSH antiserum (guinea pig; AFP-1760191) diluted to a final concentration of 1:400,000 as primary antibody. The secondary antibody is from Equitech-Bio, Inc. and was diluted to a final concentration of 1:25. The radio-immunoassay has a sensitivity of 2.0 ng/ml and less than 0.5% cross-reactivity with other pituitary hormones. When needed, the samples were diluted 5-10 fold.

Evaluation of the regularity of estrous cycle

To assess estrous cycle cessation, vaginal cytology was performed seven days after ovariectomy. After transplantation, vaginal cytology was resumed seven days post-operation and was performed daily until sacrifice. The transition from leukocytes to cornified cells at least once a week was counted as a resumed or continued cycle.

Histological analysis of the retrieved capsules and the encapsulated tissue

Immediately after retrieval of the immunoisolating capsules from mice, the capsules were fixed in Bouin's fixative at 4°C overnight and transferred and stored in 70% ethanol at 4°C. Constructs encapsulating ovarian tissue were then processed, embedded in paraffin, serially sectioned at a 5 µm thickness, and stained with hematoxylin and eosin.

To determine the stage of follicular development, follicles were classified as follows: follicles with one layer of squamous granulosa cells around the oocyte were classified as primordial follicles, a single layer of cuboidal granulosa cells - primary follicles, two or more layers of granulosa cells - a secondary follicle, and follicles with an antral cavity were classified as antral follicles.

Trichrome Staining

After retrieval of the PEG constructs from the mice, the capsules were fixed in Bouin's fixative at 4°C overnight and transferred and stored in 70% ethanol at 4°C. Hydrogels were then processed, embedded in paraffin, serially sectioned at a 5 µm thickness, and stained with Masson's Trichrome 2000 Stain Kit (American Mastertech, Inc., USA.). Capsule thickness was quantified via Image J software.

Statistics

Statistical analysis was performed using the R software. Two-sample t-tests were used to evaluate changes in hormone levels and differences in swelling ratio and storage modulus between PEG constructs. The results were considered statistically significant when $p < .05$.

RESULTS

Visco-elastic properties of PEG-VS hydrogels

To determine the physical properties of the PEG hydrogels encapsulating the ovarian tissue, we measured the equilibrium mass swelling ratio and storage modulus of 5% PEG-NPD and PEG-PD. We found that PEG-NPD, prepared via free radical photopolymerization chemistry, and PEG-PD, prepared with thiol-ene Michael type addition chemistry, had comparable swelling ratios (Figure 1A). The Q_m of PEG-PD hydrogels was 32.2, and the Q_m of PEG-NPD hydrogels was 30.2. Similarly to the swelling ratio, the storage modulus for PEG-PD hydrogels was 2403 Pa and 2876 Pa for PEG-NPD (Figure 1B,C). Specifically important for the PEG-Dual capsule, similar swelling ratios and visco-elastic properties of the two types of the hydrogels allow concentric encapsulation of the PEG-PD as a core inside a PEG-NPD shell without further modification.

Encapsulation and subcutaneous implantation of ovarian tissue

The ovarian tissue encapsulated in PEG-NPD, PEG-PD, or PEG-Dual hydrogel was completely surrounded in the respective hydrogel network (Figure 2A,D,G). For the PEG-Dual hydrogel, the ovarian tissue was encapsulated in PEG-PD core, which was surrounded by a PEG-NPD shell (Figure 2G). At the time of sacrifice, the hydrogels were easily identified and retrieved from the subcutaneous space. No difference in the appearance of the different capsules was noted. Because of the inert and non-fouling properties of PEG hydrogels, we observed minimal interaction with the host tissue at

the area around the implanted capsules (Fig 2B,E,H). At the macroscopic evaluation of the capsules, which were easily removed from the host, the ovarian tissue was visible and fully encapsulated in the center of the capsules. No signs of revascularization or cell infiltration were observed, which was the anticipated result to ensure efficient immunoisolation (Figure 2C,F,I).

Follicle development and growth in the immunoisolation capsules

We performed histological analysis of the retrieved ovarian tissue in immunoisolating capsules to investigate the growth and development of the follicles, up to 60 days post implantation. After 7 days of implantation in the immunoisolating capsule small primordial and primary follicles were found in all the capsules (Figure 3A,D,G). After 30 days of implantation multiple large antral follicles developed in the ovarian tissue implanted in PEG-PD and PEG-Dual, supporting our initial hypothesis that proteolytic degradation was essential to promote follicular growth (Figure 3B,H). We identified multiple follicles in the PEG-NPD capsule after 30 and 60 days, yet the antral follicles failed to develop an antral cavity, as demonstrated in Figure 3F. Similar to the findings at 30 days post implantation, multiple growing and fully developed antral follicles were observed in the ovarian tissue implanted in PEG-PD and PEG-Dual, but not in PEG-NPD. In agreement with our macroscopic findings, we did not find evidence of blood vessel infiltrating the implanted tissue, which further confirmed the barrier to the host by the gels.

Restoration of ovarian endocrine function

In adult mice with healthy functioning ovaries the levels of circulating FSH is below 20 ng/mL. After ovariectomy the lack of negative feedback of estradiol, normally produced in the ovarian follicles, results in increased levels of FSH that can reach 100 ng/mL. Mice in all groups had the average FSH level of 4-8 ng/mL before ovariectomy (n=16 for PEG-NPD, n=11 for PEG-PD, n=18 for PEG-Dual). After a bilateral ovariectomy, FSH levels rose significantly ($p < 0.05$) to an average of 55-71 ng/mL (n=15 for PEG-NPD, n=12 for PEG-PD, and n=16 for PEG-Dual). The rise in FSH levels is the result of low levels of circulating estradiol, confirming that the ovaries were removed and the hypothalamus-pituitary-gonad axis was disrupted. 60 days after mice received ovarian tissue encapsulated in PEG-NPD (n=6), PEG-PD (n=7), or PEG-Dual hydrogel (n=11), FSH levels decreased significantly from an average of 64 ng/mL to an average of 34.8 ($p=0.0004$), 30.5 ($p=0.028$), and 34.3 ng/mL ($p=0.01$), respectively (Figure 4A), indicating the HPG axis was restored upon implantation in all the groups.

Estrous Cycle Restoration

Estrous cycle correlates with ovulation and lasts 4-5 days in rodents. After ovariectomy the estrous cyclicity ceases, which is determined by the absence of cornified cells in the vaginal secretions. Implantation of ovarian tissue in PEG-PD restored cyclicity in 90% of the mice one week post implantation, and in 100% by the second week (Figure 4B). Restoration of cyclicity was delayed in mice that received the implants in PEG-NPD and PEG-Dual with 60% of the mice cycling 1 week after implantation, and reaching 100%

cyclicality by week 4. However, while 90% of the mice that received ovarian implant in PEG-Dual capsule continued cycling for 9 weeks, only 67% of the mice that received the PEG-NPD capsule continued cycling after 7 weeks, which correlates with the histological analysis and suggests that the follicle growth was restricted in the non-degradable capsules.

Collagen Deposition

After implantation for 30 and 60 days, PEG-PD, PEG-NPD, and PEG-Dual exhibited a thin fibrotic capsule around the respective hydrogel (Figure 5A-F). There was no significant difference in the fibrotic capsule thickness around the immunisolating capsules (Figure 5G). When comparing fibrotic capsule thickness from 30 to 60 days post-implantation, there was no significant difference in collagen deposition ($p < 0.05$), indicating the absence of a chronic inflammatory response. Cell infiltration from the host or cell migration from the encapsulated ovarian follicles was not observed in the implants. Interestingly, cells were present throughout the fibrotic capsule around the degradable hydrogel (PEG-PD) (Figure 5A), but in the case of non-degradable PEG, cells were concentrated in the narrow space between the gel and the fibrotic capsule. This finding may indicate that a degradable gel induced a different reaction with the innate immune cells compared to a non-degradable gel.

DISCUSSION

This study investigated whether the PEG-based immunoisolating capsules support the viability and function of encapsulated and implanted ovarian tissue for the purpose of restoration of ovarian endocrine function in ovariectomized mice. The results show for the first time the development and characterization of novel photo-polymerized and dual PEG based hydrogel systems. We found that PEG-VS based hydrogels support ovarian tissue and restore endocrine function for at least 60 days. Future allogeneic studies in mice and higher species will confirm whether PEG-PD and PEG-Dual constructs protect the tissue from being recognized and/or destroyed by allo-immunity.

We designed the immunoisolating capsule by tuning the physical properties of the PEG hydrogels and combining degradable and non-degradable layers to meet the numerous requirements for immunoisolation of ovarian tissue. For example, the diffusion of nutrients was achieved with low solid concentration and efficient crosslinking density of the network. The non-degradable layer of the PEG hydrogel created a physical barrier between the host and the implant. The proteolytic degradation in response to the cell-secreted proteases from the encapsulated follicles allowed the volumetric expansion of ovarian tissue. Lastly, the intermediate stiffness and inertness of the PEG hydrogel caused minimal inflammatory response at the interface of the capsule and the host.

The strategy of encapsulating the tissue grafts in encapsulating devices allows oxygen and nutrients delivery via diffusion through the hydrogel without the risk of exposure to the immune cells. These properties may be useful to prevent rejection of

tissue allografts which inevitably occur when the tissue is directly transplanted. The tunability of PEG hydrogels allows excellent control over pore size of the network formed around the encapsulated tissue. Ovarian tissue encapsulated in PEG-PD, PEG-NPD and the PEG-Dual capsule survived the encapsulation and the implantation for 60 days. The histological sections of the retrieved tissue demonstrated no evidence of necrosis and appeared normal with phenotypically healthy follicles. Further, in the dual capsule we matched the swelling ratio and storage moduli of each layer, which allowed us to co-encapsulate several layers of hydrogels having similar properties. The degradable core around the encapsulated ovarian tissue surrounded by a non-degradable shell interfacing with the host isolated the tissue from the host environment, while still allowing diffusion and promoting survival of the tissue.

Ovarian follicles exhibit dynamic growth during the hormonal phases, necessitating a need for a material with viscoelastic properties that either degrades in response to follicle secreted proteases or can mechanically withstand the follicle expansion. Our previous study using alginate as an immunoislator for ovarian tissue demonstrated that the viscous properties of alginate were insufficient to support the follicle expansion, and either excessively compressed the tissue or failed to maintain the protective layer²⁶. Shikanov et al. demonstrated that a proteolytically degradable PEG-VS hydrogel system was conducive for the development of ovarian follicles as they can grow, mature, and respond to circulating gonadotropins in culture¹⁹. Here, we proposed to encapsulate the ovarian tissue in viscoelastic PEG hydrogel and determine whether the proteolytic degradation of the matrix was essential for ovarian tissue survival and

function. When implanted in mice for 7, 30, and 60 days, all PEG constructs supported ovarian tissue survival and secondary and antral follicles were present in the retrieved implants. FSH levels in mice with ovarian tissue encapsulated in PEG-NPD, PEG-PD, and PEG-Dual significantly decreased 60 days post-implantation compared to pre-implantation levels ($p < 0.05$), indicating the reversal of the ovariectomized phenotype and restoration of the ovarian endocrine function. The restoration of the estrous cycle and the decrease in FSH levels proved that the tissue encapsulated in the construct responded to the circulating gonadotropins and the encapsulated follicles secreted estradiol creating a negative feedback loop in the HPG axis. The histological evaluation of the encapsulated tissue indicated that PEG-PD was superior in terms of supporting tissue viability and function compared to PEG-NPD. PEG-PD degraded in response to the secreted proteases from cells, providing a supporting network without exerting a compressive force back on the tissue in a way PEG-NPD does. However, PEG-PD cannot solely serve as an efficient immunoislator and eventually would degrade exposing the tissue to the host immune system. Co-encapsulation of a degradable PEG-PD core in a non-degradable PEG-NPD shell demonstrated successful restoration of ovarian endocrine function similar to PEG-PD alone with the possibility for no risk of rejection. As PEG-PD degrades over time, the outer layer of PEG-NPD is crucial to protect the implanted tissue for allogeneic implantations. The inclusion of a degradable core provides the biomimetic microenvironment for the encapsulated ovarian tissue while the PEG-NPD outer shell provides protection from the immune cells in the host. In the current study, we demonstrated that the ovarian tissue encapsulated in PEG-Dual

hydrogel remains healthy long-term and restoration of endocrine function occurs as indicated by the continuation of the estrous cycle. Corresponding to this observation we observed a significant decrease in FSH levels compared to the pre-implantation levels.

Synthetic biomaterials, such as PEG hydrogels, are an attractive platform for protein and cell delivery because of their low inflammatory index^{21,22}. PEG hydrogels are one of the most commonly used synthetic materials for islet immunoisolation, for example. Multiple reports demonstrated that islets encapsulated in PEG remained viable and maintained normoglycemia^{16-18,27}. PEGylated membranes also protected islets from cytokine induced inflammation and destruction *in vitro*¹⁵. Similarly, the implanted PEG-based capsules with encapsulated ovarian tissue described here did not cause an excessive inflammatory reaction. Our *in vivo* studies demonstrated a thin collagen capsule formation, which correlates with a minimal inflammatory response characteristic to the inert properties of PEG hydrogels. Importantly, we did not observe infiltration of cells or blood vessels from the host, which further confirmed the efficiency of the tested hydrogels as establishing a barrier between the tissue and the host environment.

ACKNOWLEDGEMENTS

This work was supported by The Hartwell Foundation (14-PAF00981), the National Institute of Biomedical Imaging and Bioengineering to AS and MC (R01 EB022033), and the National Science Foundation Graduate Research Fellowship Program (DGE 1256260) to JRD.

REFERENCES

1. Ginsberg JP. New advances in fertility preservation for pediatric cancer patients. *Curr. Opin. Pediatr.* 2011; 23: 9-13.
2. Chiarelli AM, Marrett LD, Darlington G. Early menopause and infertility in females after treatment for childhood cancer diagnosed in 1964-1988 in ontario, canada. *Am J Epidemiol.* 1999; 150(3): 245-54.
3. Hershlag A, Rausch ME, Cohen M. Part 2: Ovarian failure in adolescent cancer survivors should be treated. *J Pediatr Adolesc Gynecol.* 2011; 24(2): 101-103.
4. Thibaud E, Rodriguez-Macias K, Trivin C, Esperou H, Michon J, Brauner R. Ovarian function after bone marrow transplantation during childhood. *Bone Marrow Transplant.* 1998 Feb; 21(3): 287-90.
5. Waring AB, Wallace WH. Subfertility following treatment for childhood cancer. *Hosp Med.* 2000 Aug; 61(8): 550-7.
6. Nieman CL, Kinahan KE, Yount SE, Rosenbloom SK, Yost KJ, Hahn EA, Volpe T, Dilley KJ, Zoloth L, Woodruff TK. Fertility preservation and adolescent cancer patients: Lessons from adult survivors of childhood cancer and their parents. *Cancer Treat Res.* 2007; 138: 201-17.
7. Hudson MM, Oeffinger KC, Jones K, Brinkman TM, Krull KR, Mulrooney DA, Mertens A, Castellino SM, Casillas J, Gurney JG, Nathan PC, Leisenring W, Robison LL, Ness KK. Age-dependent changes in health status in the childhood cancer survivor cohort. *J Clin Oncol.* 2015; 33(5): 479-491. PMID: PMC4314595.
8. Mariotto AB, Rowland JH, Yabroff KR, Scoppa S, Hachey M, Ries L, Feuer EJ. Long-term survivors of childhood cancers in the united states. *Cancer Epidemiol Biomarkers Prev.* 2009; 18(4): 1033-1040.
9. Phillips SM, Padgett LS, Leisenring WM, Stratton KK, Bishop K, Krull KR, Alfano CM, Gibson TM, de Moor JS, Hartigan DB, Armstrong GT, Robison LL, Rowland JH, Oeffinger KC, Mariotto AB. Survivors of childhood cancer in the united states: Prevalence and burden of morbidity. *Cancer Epidemiol Biomarkers Prev.* 2015; 24(4): 653-663. PMID: PMC4418452.
10. Robison LL, Hudson MM. Survivors of childhood and adolescent cancer: Life-long risks and responsibilities. *Nat Rev Cancer.* 2014; 14(1): 61-70.

11. Dolmans MM, Luyckx V, Donnez J, Andersen CY, Greve T. Risk of transferring malignant cells with transplanted frozen-thawed ovarian tissue. *Fertil Steril*. 2013; 99(6): 1514-1522.
12. Kniazeva E, Hardy AN, Boukaidi SA, Woodruff TK, Jeruss JS, Shea LD. Primordial follicle transplantation within designer biomaterial grafts produce live births in a mouse infertility model. *Sci Rep*. 2015; 5: 17709. PMID: PMC4668556.
13. Dolmans MM, Marinescu C, Saussoy P, Van Langendonck A, Amorim C, Donnez J. Reimplantation of cryopreserved ovarian tissue from patients with acute lymphoblastic leukemia is potentially unsafe. *Blood*. 2010; 116(16): 2908-2914.
14. Boettler T, Schneider D, Cheng Y, Kadoya K, Brandon EP, Martinson L, and Herrath MV. Pancreatic tissue transplanted in TheraCyte™ encapsulation devices are protected and prevent hyperglycemia in a mouse model of immune-mediated diabetes. *Cell Transpl*. 2015; 25:609–614.
15. Nabavimanesh MM, Hashemi-Najafabadi S, and Vasheghani-Farahani E. Islets immunoisolation using encapsulation and PEGylation, simultaneously, as a novel design. *J. Biosci. Bioeng*. 2015;119:486–491.
16. Weber, L. M., C. Y. Cheung, and K. S. Anseth. Multifunctional pancreatic islet encapsulation barriers achieved via multilayer PEG hydrogels. *Cell Transpl*. 2008;16:1049–1057.
17. Cruise GM, Hegre OD, Lamberti FV, Hager SR, Hill R, Scharp DS, Hubbell JA. In vitro and in vivo performance of porcine islets encapsulated in interfacially photopolymerized poly (ethylene glycol) diacrylate membranes. *Cell Transplant*. 1999; 8: 293-306.
18. Schweicher J, Nyitray C, Desai TA. Membranes to achieve immunoprotection of transplanted islets. *Front Biosci (Landmark Ed)*. 2014; 19:49-76.
19. Shikanov A, Smith RM, Xu M, Woodruff TK, Shea LD. Hydrogel network design using multifunctional macromers to coordinate tissue maturation in ovarian follicle culture. *Biomaterials*. 2011;32(10):2524-31.
20. Kim J, Perez AS, Clafin J, David A, Zhou H, Shikanov A. Synthetic hydrogel supports the function and regeneration of artificial ovarian tissue in mice. *npj Regenerative Medicine*. 2016;1: doi:10.1038/npjregenmed.2016.10
21. Tibbitt MW, Anseth KS. Hydrogels as extracellular matrix mimics for 3D cell culture. *Biotechnol Bioeng*. 2009;103(4):655-63.
22. Bryant SJ, Bender RJ, Durand KL, Anseth KS. Encapsulating chondrocytes in degrading PEG hydrogels with high modulus: engineering gel structural changes to facilitate cartilaginous tissue production. *Biotechnol Bioeng*. 2004;86:747-55.
23. Williams CG, Malik AN, Kim TK, Manson PN, Elisseff JH. Variable cytocompatibility of six cell lines with photoinitiators used for polymerizing hydrogels and cell encapsulation. *Biomaterials*. 2005;26:1211-1218.
24. Hao Y, Shih H, Munoz Z, Kemp A, Lin C. Visible light cured thiol-vinyl hydrogels with tunable degradation for 3D cell culture. *Acta Biomater*. 2014;10(1):104-14.

25. Shih H, Lin CC. Crosslinking and degradation of step-growth hydrogels formed by thiol-ene photo-click chemistry. *Biomacromolecules*. 2012;12(7):2003-2012.
26. David A, Day JR, Cichon AL, Lefferts A, Cascalho M, Shikanov A. Restoring Ovarian Endocrine Function with Encapsulated Ovarian Allograft in Immune Competent Mice. *Annals in Biomedical Engineering*. 2017;45(7):1685-1696.
27. Headen DM, Aubry G, Lu H, Garcia AJ. Microfluidic-based generation of size-controlled, biofunctionalized synthetic polymer microgels for cell encapsulation. *Adv Mater* . 2014;6:3003-8.

Figures Legend:

Scheme 1: Representation of encapsulating ovarian tissue in a PEG-Dual capsule with a PEG-PD core and PEG-NPD outer shell

Figure 1: (A) Swelling ratio (n=5 for all compositions) and (B) storage modulus of 5% PEG-PD (n=3) and PEG-NPD (n=4). (C) Illustration of storage modulus and loss modulus of 5% PEG-PD and 5% PEG-NPD. All data reported A,B is mean \pm SD.

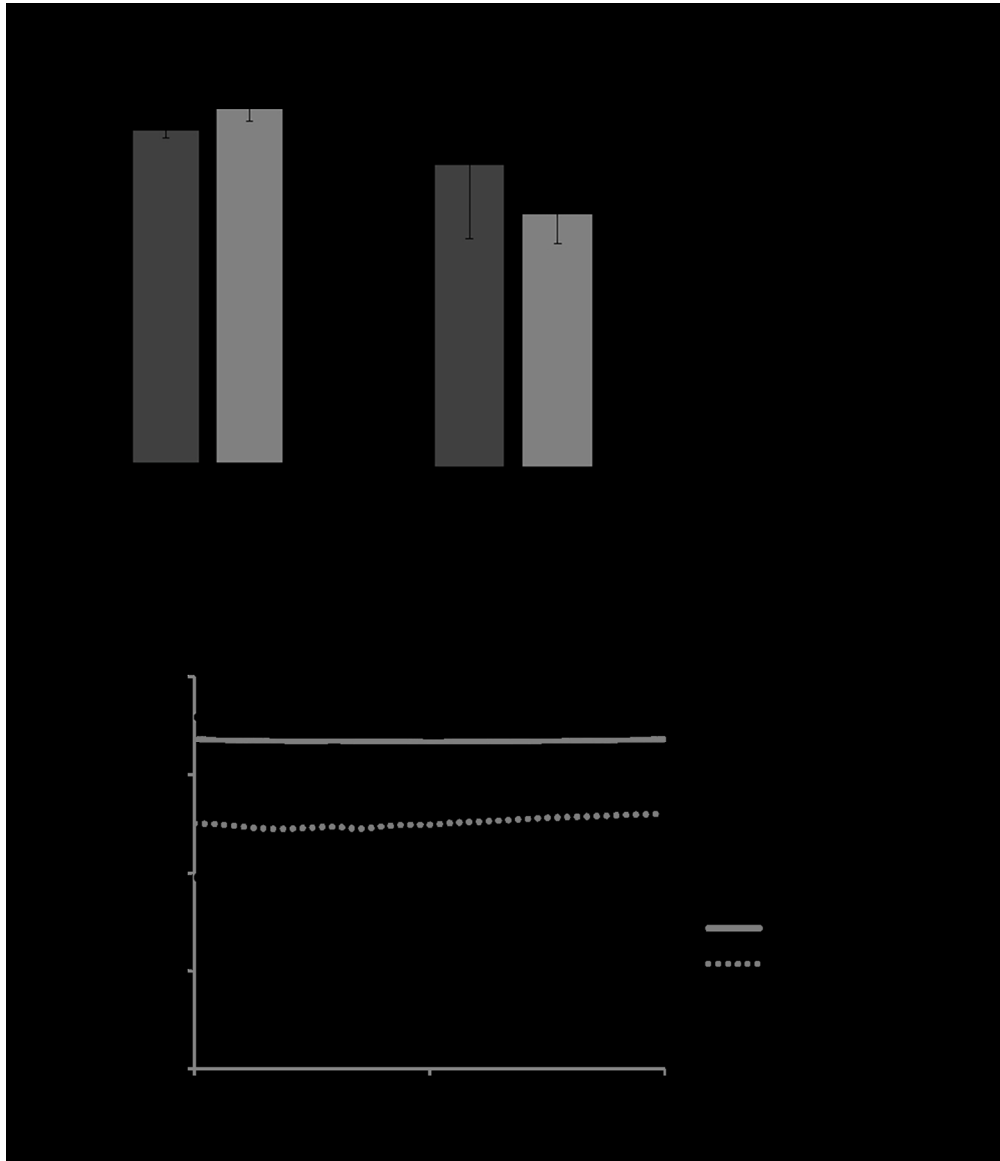
Figure 2: Macroscopic images of PEG-VS hydrogels before and after implantation. (A) Ovarian tissue encapsulated in PEG-PD, (B) PEG-PD at the time of sacrifice, (C) PEG-PD after removal, (D) Ovarian tissue encapsulated in PEG-NPD, (E) PEG-NPD at the time of sacrifice, (F) PEG-NPD after removal, (G) Ovarian tissue encapsulated in PEG-Dual, (H) PEG-Dual at the time of sacrifice, (I) PEG-Dual after removal. White dotted circle indicates the localization of the hydrogel on the mice. Solid black arrows indicate encapsulated ovarian tissue. Dashed black arrows indicate the border of PEG-PD and solid white arrows indicate the border of PEG-NPD. Magnification 5X (A, D, G)

Figure 3: Histological image of ovarian tissue encapsulated: in PEG-PD (A) showing primordial (*) and primary follicles (**) in 7 day implants (n=3 mice), (B), (C) showing secondary (***) and antral follicles (****) in 30 (n=4 mice) and 60 day (n=7 mice) implants respectively, PEG-NPD implants showing primordial and secondary follicles (D, E, F) after 7 (n=8 mice), 30 (n=4 mice) and 60 (n=6 mice) days respectively and PEG-Dual implants showing secondary (G) and antral (H,I) follicles in 7 (n=3 mice), 30 (n=4 mice) and 60 (n=11 mice) day implants respectively. (P)

indicates the encapsulating PEG hydrogel. "ac" indicates antral cavity. Magnification 10X **(B,C,E)**, 20X **(A,D,F,G,H,I)**.

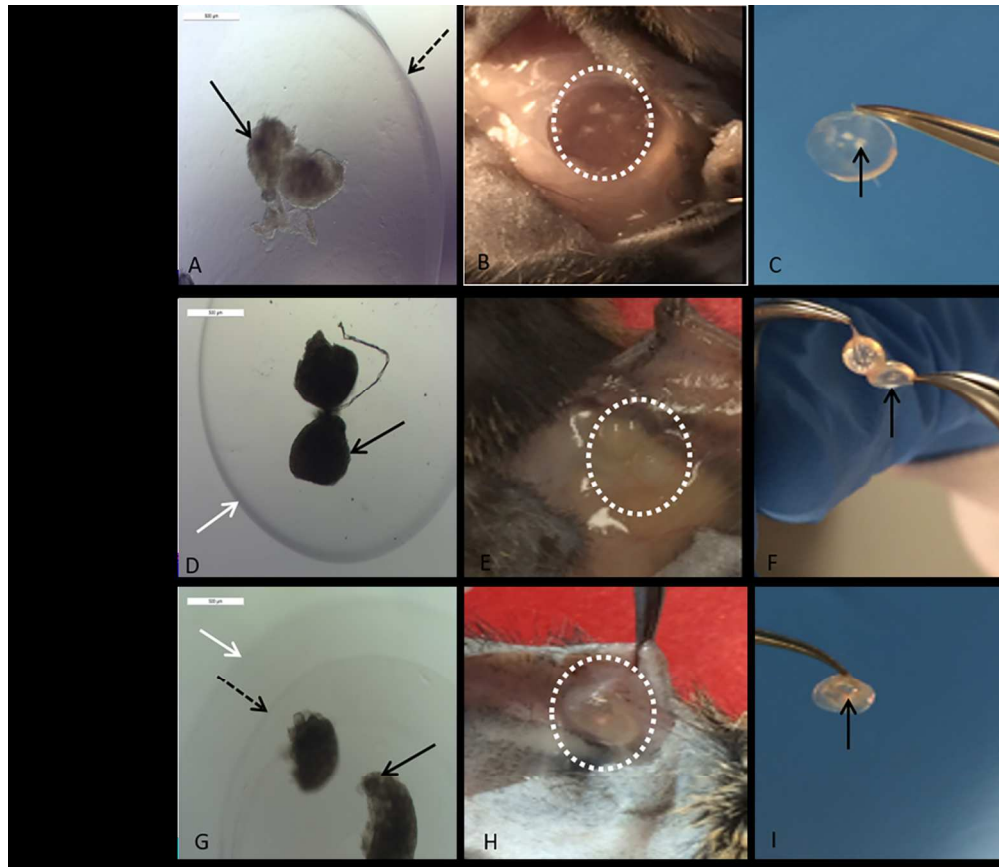
Figure 4: (A) FSH levels of mice receiving ovarian tissue encapsulated in PEG-NPD, PEG-PD, and PEG-Dual before ovariectomy, after ovariectomy, four weeks post-implantation, and sixty days post-implantation. An asterisk (*) denotes a significant difference ($p < 0.05$) between pre-ovariectomy levels and the designated group. Significance was determined by a two-sample T-test. **(B)** Cyclicity observed in mice implanted with D-PEG, ND-PEG and PEG-Dual in the syngeneic model. Presence of a change between leukocytes and cornified cells at least once per week was deemed continuation of estrous cycles.

Figure 5: Trichrome staining of fibrotic capsule around PEG-NPD, PEG-PD, and PEG-Dual after 30 days **(A, B, C)** and 60 days **(D, E, F)** subcutaneous implantation in mice. An asterisk (*) indicates the PEG hydrogel. Magnification 40X. **(G)** Quantification of fibrotic capsule thickness around immunisolating devices after 30 and 60 days using Image J. n=10 for PEG-PD, PEG-NPD, and PEG-Dual.



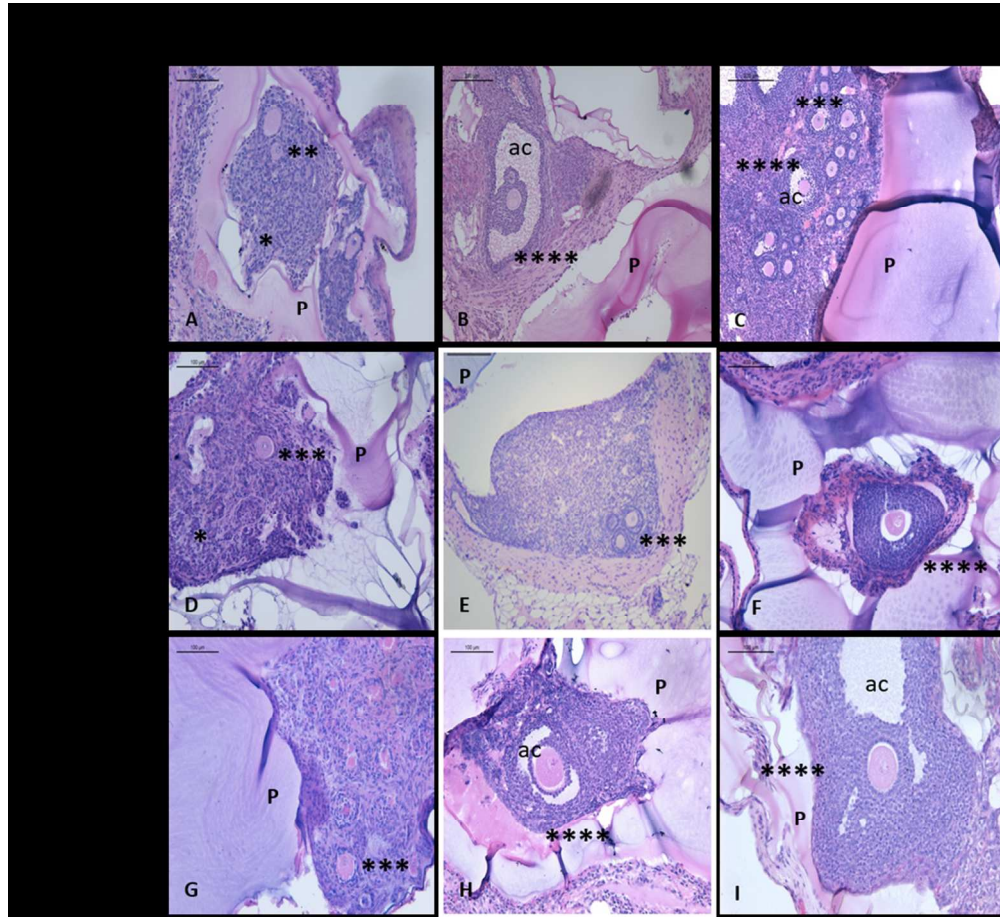
101x117mm (300 x 300 DPI)

Au:



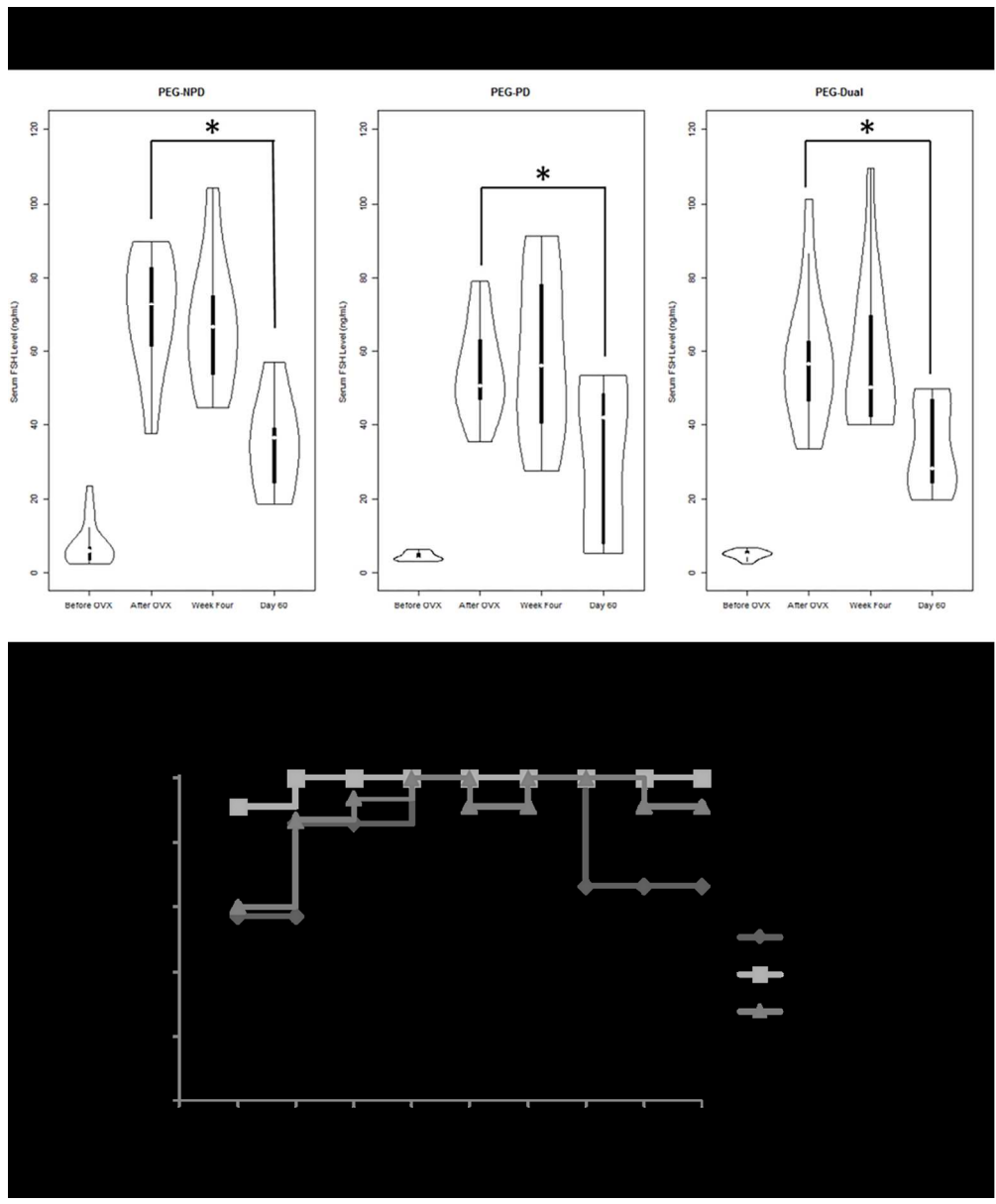
101x87mm (300 x 300 DPI)

Autho!



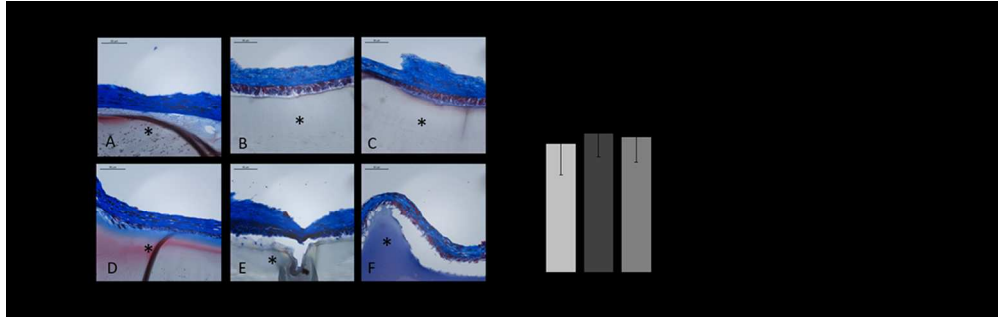
101x93mm (300 x 300 DPI)

Autho



101x122mm (300 x 300 DPI)

AU



101x32mm (300 x 300 DPI)

Author Man



101x18mm (300 x 300 DPI)

Author Manuscript